Interaction of zinc peroxide nanoparticle with fibroblast cell

Bharti Sharma[1], Nahar Singh[2], Ram P. Tandon[1], Ajit K. Mahapatro[1*]

[1]*Department of Physics and Astrophysics, University of Delhi, Delhi, 110007, India*
[2]*Analytical Chemistry Division, CSIR-National Physical Laboratory, Dr. K. S. Krishnan Marg, New Delhi, 110012, India*

[*]Corresponding author: Tel: (+91) 9871074984; E-mail: amahapatro@physics.du.ac.in

Received: 09 April 2016, Revised: 23 August 2016 and Accepted: 17 April 2017

DOI: 10.5185/amp.2017/708
www.vbripress.com/amp

Abstract

This work demonstrates the structural interaction of the as-synthesized zinc peroxide (ZnO_2) nanoparticles with fibroblast cells (FBC). The ZnO_2 nanoparticles (ZNP) of desired sizes (10-20 nm) are synthesized, and the purity and structural confirmations are studied using various imaging and spectroscopic techniques. FBC (buffalo) lines are cultured in Dulbecco's modified Eagle's medium (DMEM) supplemented with 10% fetal bovine serum and penicillin (100 μg/mL), and with non-essential amino acid and vitamin as additional ingredients, followed by incubation at 37°C with continuous purging of the chamber using 5% CO_2. The fluorescent microscopic images are captured for the initial healthy and cultured FBCs, and after pouring the nanoparticles in the cultured FBCs. Healthy cell-growth is noticed during the cell culture process suggesting the formation of ZNP-FBC complexes without contamination and coagulation. After allowing the interaction of ZNPs with the FBCs, the presence of ZNPs only on the cell sites are observed without coagulation of ZNPs in the cell areas, suggesting the selective interference of ZNPs on the surface of the grown cell. The understanding of the interaction process of the ZNPs with the living cell, would provide the practical utilization of the ZNPs in nanomedicine and nano-drug delivery.

Keywords: Zinc peroxide (ZnO_2) nanoparticle (ZNP), fibroblast cell (FBC), ZNP-FBC interaction, cell metabolism, nano-drug delivery.

Introduction

The gain in knowledge on the interaction of nanomaterials with living cell could provide information about the possible accessibility to interfere with the living cell machinery without potentially triggering the side effects and toxicity. The nanoparticle and cell interaction is a crucial issue in nanomedicine and nanotoxicology. The ability of the molecular sized nanoparticles to invade the living cells through the cellular endocytosis machinery is an interesting aspect for identifying targeting cells and transporting essential drugs into the biological entity through nanoparticle processing. Utilization of nanoparticles in therapeutic and/or diagnostic agents for biomedical applications and for intracellular targets, it is requires the nanomaterials to enter the living cell. The advantages of the nanoparticles are their small size with unique size dependent properties, high reactivity and large surface area that allow them to interact with cell components.

The currently available diagnostic tools in clinical practice including magnetic resonance imaging, ultrasound, radio imaging, X-ray imaging, optical imaging, etc., do not facilitate comprehensive diagnostic visualization about a diseased cell/tissue/organ **[1-3]**. Investigation for understanding the interaction between the nanomaterials and living cell could lead to practical biomedical applications of nanomaterials. The mechanisms involved at the nano–bio interface comprises of the dynamic physicochemical interactions, kinetics and thermodynamic exchanges between nanomaterial surfaces and the surfaces of biological components including proteins, membranes, phospholipids, endocytic vesicles, organelles, DNA, and biological fluids. The factors describing the dynamical interaction includes, (i) the nanoparticle surface with physicochemical compositions, (ii) stress at the nanoparticle-cell interface due to the changes during the particle interaction with the surrounding medium, and (iii) interaction of nanoparticle and substrate at the contact zone of the biological entity.

The physico-chemical features of the nanoparticles are the determining factors for the nanoparticle-living cell interactions and consequently influence cell behaviour. The size and shape of the nanomaterials and chemical functionalities on the surface play a critical role in binding the nanomaterials to cell membrane and subsequent cellular uptake **[4-6]**. This motivates pursuing

research towards the biological interference of nanoparticles and development of multi-model diagnostic probes that could facilitate the combination dignostics, preferably covering both the anatomical and physiological aspect of various disease **[7-8]** including the deadly cancer.

The advantage of nanoparticles such as ultra-small size, ease in synthesis, and biocompatibility are suitable for a variety of medical applications **[9-11]**. Nanoparticles present ideal platform for the fabrication of multimodal agents [12-13]. The structural nanoparticles, such as silica, biodegradable polymers, etc., which provide a matrix for hosting one or multiple active agents, including smaller functional nanoparticles with unique physical parameters defined in metallic and inorganic nanoparticles, quantum dots, etc. The surface of the nanomaterials can be aptly functionalized to enhance their circulation in the blood and targeting specificity **[14-16]**. Various kind of functional nanoparticles available, zinc oxide, iron oxide which have the most promising application in the field of medicine **[17-20].**

In a given medium, the most important nanoparticle characteristics that determine the surface properties are the material's chemical composition, surface functionalization, shape and angle of curvature, porosity and surface crystalinity, heterogeneity, roughness, and hydrophobicity or hydrophilicity **[21-23]**. Other quantifiable properties, such as effective surface charge (zetapotential), particle aggregation, state of dispersion, stability/biodegradability, dissolution characteristics, hydration and valence of the surface layer, are determined by the characteristics of the suspending media, including the ionic strength, pH, temperature and the presence of large organic molecule **[24]**. The media and bio-entity could also induce large scale changes in the nanomaterials properties including nanoparticle dissolution, ion leaching, phase transformation and agglomeration. The zinc peroxide nanoparticles have broad antibacterial activities against bacteria and fungus with biocompatible and non-toxic.

In this work, we have synthesized highly pure zinc peroxide (ZnO_2) nanoparticles (ZNPs) and demonstrated the interaction of the ZNPs with the Fibroblast cells (FBCs). The high purity of the ZNPs are characterized using advanced imaging and spectroscopic tools.

Experimental

Materials

The required chemicals zinc acetate, zinc nitrate, zinc sulphate, zinc chloride, sodium hydroxide, hydrogen peroxide, glycerol, polyvinaylpyrrilodone (PVP), tetra ethylamine (TEA), 3- mercaptopropoinic acid (MPA), acetone, methanol, ethanol etc. used in the synthesis of ZnO_2 of analytical grade and are purchased from E. Merck. Hydrochloric acid (35%) of GR Grade used after purify through sub–boiling distillation quartz glass device. De-ionized water used of 18.2 MΩ resistivity for all experimental work is prepared with Millipore milli-Q element water purification system, USA. The 1µg/ml standard stock solution of ZnO_2 is prepared in DMEM media. The pipettes, beakers, volumetric flask of various capacities used are of Borosil glass works India limited. The pipettes and volumetric flasks were calibrated prior to analysis following international standard procedure and protocol **[25]**. All the wet chemical digestion and dilution work is carried out in a laminar flow clean bench.

Synthesis of ZnO_2 nanoparticles

10 gm of zinc salt was dissolved in dilute ammonia solution and further diluted to 200 ml in 1:1 ratio of methanol and water. Varying quantity of PVP is added to this solution achieve desired particles size of ZnO_2. Further dilute hydrogen peroxide solution is added upto complete precipitation in solution is achieved maintain the pH of 9-11 at 50-55 °C temperature and stirred on magnetic stirrer for 1 hour. The precipitate formed is centrifuged at 8000 rpm followed by washing with de-ionized water and methanol for several time. Finally, the precipitate is dried at 105 ºC in an oven upto complete dryness **[26]**.

Cell culture and counting

The cell lines from different origins of tissues are utilized. Fibrobalast cell is grown in Dulbecco's modified Eagle's medium (DMEM) supplemented with 10% fetal bovine serum (FBS) and 1% penicillin/streptomycin. Cell suspension is added to 25 cm^2 vials and transferred into an incubator at 37 °C with 5% CO_2. After incubation, the cells trypsinized with 1% trypsin solution and rushed down from the bottom of 25 cm^2 vials when they are in a semi confluent state and still in log phase of growth. For analyzing the cell stability with various nanoparticles the cell was trypsinized and resuspended in fresh media, one day prior to treatment, 100000 cells per 1mL fresh media are added to each well of a sterilized 24-well plate, and transferred to the incubator for attachment and overnight growth. The next day, three different dosages of the various samples are added to the cells at a confluency of 70-80% and swirl mixed, transferred back to the incubator. After three days of incubation, the plate is taken out, and the cells in each well are washed three times with sterile PBS. The density of cell is estimated by counting the numbers using hemocytometer.

Characterization

The ZnO_2 nanoparticles are characterized for the crystallographic phases by X-ray diffraction, XRD, (Bruker) model AXS D8 Advance Diffractometer. The data collection and analysis are carried out using $Diffrac^{plus}$ software, while the diffractogram is rerecorded using CuKα radiation with a graphite monochromator in the diffracted beam. The shape and size of

nanoparticlesare characterized using transmission electron microscopy, FEI, Netherland make, model F-30 G2 STWI. The cells are visualized under a fluorescent inverted microscope and photographed using a Nikon DIGITAL SIGHT DS-F11 Camera, NikonTS-100 (Nikon, Japan).

Results and discussion

The surface morphology of the ZnO_2 nanoparticle is imaged by using LEO 440 scanning electron microscope (SEM) at 5 kX magnifications and is shown in **Fig. 1**, which shows hexagonal morphologies of the as-synthesized ZNPs.

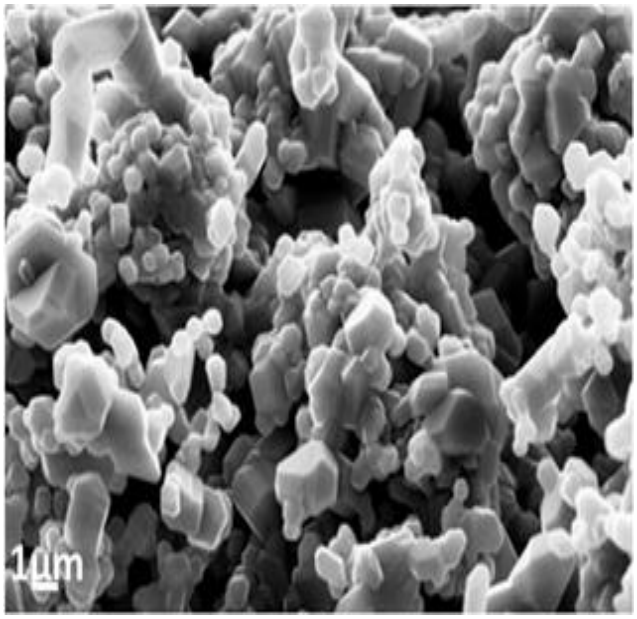

Fig. 1. SEM image of the as-synthesized ZnO_2nanocomposite

The EDX measurements, as represented in **Fig. 2**, recodes the contents of O and Zn of synthesized samples. The table in the inset of **Fig. 2**, shows the composition of the elemental O and Zn content present in the synthesized ZnO_2 nanocomposites, confirming the stoichiometric ratio of 1:2.

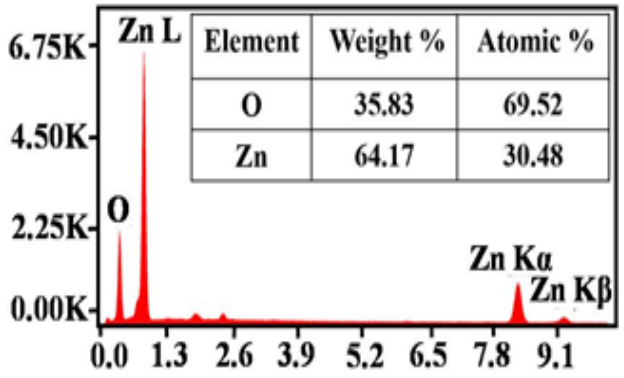

Fig. 2. Energy dispersive X-ray (EDX) spectroscopy for synthesized ZnO_2 nanocomposite. The table in the inset shows the composition of the elemental O and Zn content present in the synthesized nanocomposites.

The crystallography study of ZNPs is recorded using XRD patterns and a representative XRD pattern of the as-synthesized ZnO_2nanoparticles 2θ in the range of 20° to 80°is shown in **Fig. 3**. The observed diffraction pattern agrees well with the JCPDS data PDF # 13-0311, confirms the formation of a single-phase ZnO_2 nanoparticle. The crystallite size of 6±2 nm is estimated for the currently developed as-synthesized ZNPs using Scherrer's equation [**27**]. ZNP pellets are formed by the KBr Pellet technique of gentle mixing of ZnO_2 species with 300mg of KBr powder and compressed into discs at a force of 13kN for 5min using a manual tablet presser.

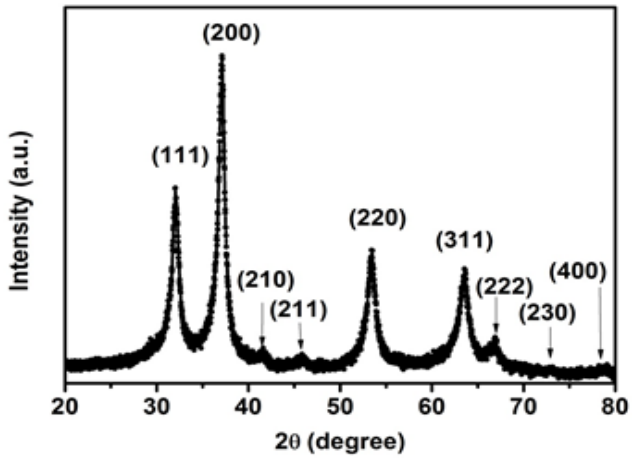

Fig. 3. XRD pattern of the as-synthesized ZnO_2nanocomposites having crystallite size 6±2 nm.

FTIR spectra of the resulting ZNP is recorded at room temperature and is plotted in **Fig. 4.** This shows the characteristic peak ZnO_2 absorption at 435–445cm^{-1} for the ZNPs. The peaks at 1040–1070cm^{-1}, 3200–3600cm^{-1}, and 1630–1660 cm^{-1} are originated from the O–O bands, water O–H stretching vibration mode, and OH bending of water, respectively. This indicates the presence of small amount of water adsorbed on the nanoparticles surface. Also, the existence of CO_2 molecule in the ambient air, there is FTIR peak at around 2360cm^{-1}.

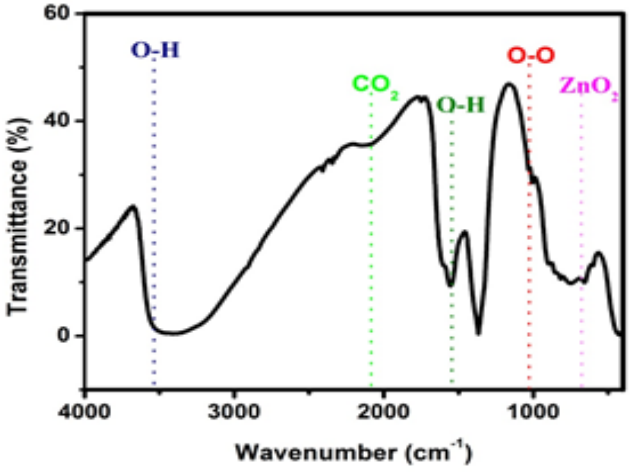

Fig. 4. FTIR spectra of the as-synthesized ZnO_2nanoparticles absorbed at 435–445cm^{-1}

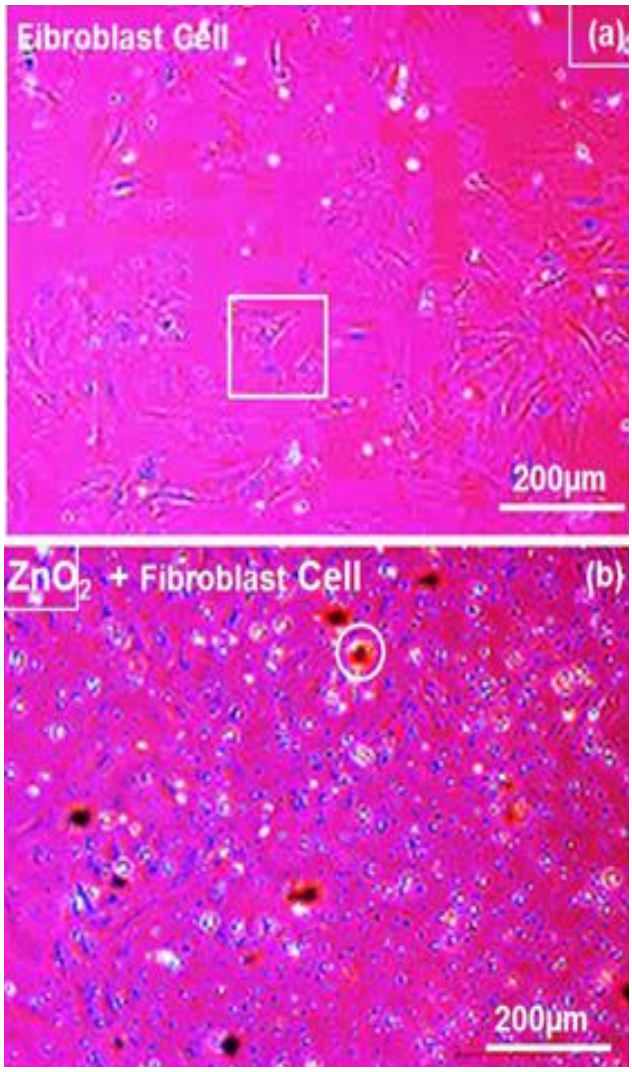

Fig. 5. Fluorescent Microscopic images of (a) fibroblast cell (b) ZnO_2+ fibrobalast cell.

The phase contrast images of living cells interaction with ZnO_2 NPs. are captured using fluorescent microscopy. The fibrobalast cells are visualized as growing and reproducing after the ZNPs are directly in contact with FBCs (**Fig. 5**). These contrast images are divided in two part (a) is cell grown in media without nanoparticles, which represent in squre box, (b) ZNPs nanoparticle are attached with the surface of the grown cells after pouring of the ZnO_2 nanoparticles in culture FBCs that interact with the cell without coagulation and without bacterial infection, after one day the ZNPs are remaining in the same position of the cell surface, which shows the cell growth with the ZNPs nanoparticles are evenly directly contact which marked in circle).

This suggests that the ZnO_2 nanoparticles are biocompatible and biosafe for the FBC cell lines. We have reported the first cellular level study on the biocompatibility and biosafety of ZnO_2 NPs and second is attachment with the cells. Fibarobalast cell line showed complete biocompatible to ZnO_2 nanostructures at low concentration.

Conclusion

This work demonstrates the initial cellular level study on the biocompatibility and biosafety of as-synthesized ZnO_2 nanoparticles. Cell lines from different origins of tissues are utilized to study the interaction of ZNP with the live cells. The Fibarobalast cell lines show stable and complete biocompatibility to the ZnO_2 nanostructures interaction. This study shows the ZNPs could be applied in vivo biomedical science and engineering applications at normal concentration range.

Acknowledgements

The authors are grateful to Prem Singh Yadav of CIRB, Hisar, India,for encouragement and providing permission to pursue the cell culture experiments in the institute. The authors would like to thank the Life Science Reserch Board of Defence Research and Development Organization (DRDO), Delhi, India, for providing fellowship to BS and for allocating extramural research funding to pursue this research work.

References

1. Prasad, P. N.; Nanotechnology for Biophotonics: Bionanophotonics. Introduction to Bionanophotonics; John Wiley & Sons: Hoboken, NJ, USA, **2004**; 520. **DOI:** 10.1002/0471465380.ch15
2. James, M. L.; Gambhir, S.S.; *Physiol. Rev*. **2012**, *92*, 897. **DOI:** 10.1152/physrev.00049.2010
3. Higgins, L .J.; Pomper, M.G.; *Semin. Oncol*. **2011**, *38*, 3. **DOI**: 10.1016/j.ejca.2014.01.004
4. Verma, A.; Stellacci, F.; *Small Weinh. Bergstr. Ger*. **2010,** *6*, 12. **DOI:** 10.1016/j.nantod.2015.07.002
5. Shang, L.; Nienhaus, K.,; Nienhaus, G.U.; *J. Nanobiotechnol*. **2014**, *12*, 5. **DOI:** 10.1186/1477-3155-12-5
6. Zhao, F.; Zhao, Y.; Liu, Y.; Chang, X.; Chen, C.; Zhao, Y.; *Small Weinh. Bergstr. Ger*. **2011**, *7*, 1322. **DOI:** 10.1155/2015/961208
7. Lee, D. E.; Koo, H.; Sun, I. C.; Ryu, J. H.; Kim, K.; Kwon, I. C.; *Chem. Soc. Rev*. **2012**, *41*, 2656. **DOI:** 10.1039/C2CS15261D
8. Swierczewska, M.; Lee, S.; Chen, X.; *Mol. Imaging*. **2011**, *10*, 3. **DOI:** NIHMS454982
9. Koo, Y. E.; Fan ,W.; Hah, H.; Xu, H.; Orringer, D.; Ross, B.; Rehemtulla, A.; Phillbert, M. A.; kopelman, R.; *Appl. Opt*. **2007,** *46*, 1924. **DOI:** 10.1039/c4ra00331d
10. Doane, T. L.; Burda, C. Chem.Soc.Rev. **2012**, *41*, 2885. **DOI:** 10.1039/C3CC47124A
11. Sharma, P.; Singh, A.; Brown, S. C.; Bengtsson, N.; Walter, G. A.; Grobmyer, S. R.; Lwakuma.; Santra, S.; Scott, E.W.; Moudgil, B. M.; + **2010**, *624*, 67. **DOI:** 10.1039/C3TB20859A
12. Yong, K.T.; Roy, I.; Swihart, M. T.; Prasad, P.N.; *J. Matter. Chem*. **2009**, *19*, 4655 **DOI:** 10.1021/nn8008933
13. Parveen, S.; Misra, R.; Sahoo, S. K.; *Nanomedicine*. **2012**, *8*, 147 **DOI:** 10.1016/j.nano.2011.05.016.
14. Davis, S. S.; *Trends Biotechnol*.. **1997**, *15*, 217 **DOI:** 9183864 [PubMed]
15. Ruoslahti, E.S.; Bhatia N.; Sailor, M. J.; *J. Cell Biol.* **2010**, *188*, 759. **DOI:** 10.1083/jcb.200910104
16. Gong, Y. K..; Winnik, F. M.; *Nanoscale*. **2012**, *4*, 360. **DOI:** 10.1039/c1nr11297j
17. Vasir, J. K., Labhasetwar, V.; *Technol. Cancer Res. Treat*. **2005**, *4*, 363. **DOI:** 16029056 [PubMed]
18. Li, Z.;, Yang, R.; Yu, M.; Bai, F.; Li, C.; Wang, Z. L.; *J. Phys. Chem. C*. **2008**, *112*, 20114. **DOI:** 10.1021/jp808878p

19. Gupta, A. K., Gupta, M.; *Biomaterials*, **2005**, *26*, 3995.
DOI: 10.1016/j.biomaterials.2004.10.012
20. MeCarthy, J. R.; Weissleder R.; *Adv. Drug Delivery Rev.* **2008**, *60*, 1241.
DOI: 10.1016/j.addr.2008.03.014
21. Nel, A.; Xia, T.; Madler, L.; Li, N. *Science*. **2006**, *311*, 622–627**.**
DOI: 10.1186/1743-8977-2-8
22. Oberdorster, G. *et al*.; *Part. Fibre Toxicol.***, 2005,** *2*, 8
DOI: 10.1186/1743-8977-2-8
23. Vertegel, A. A.; Siegel, R. W.; *Langmuir*, **2004,** *20*, 6800–6807**.**
DOI: 10.1021/la0497200 PMID:15274588
24. Sigmund, W.; Pyrgiotakis, G.; Daga, A. *Chemical Processing of Ceramics* (CRC, **2005**).
DOI: ISBN- 1574446487
25. Singh, N et al, *Chalcogenide Lett.*, **2010**, *4*, 7.
26. Singh, N.; Rashmi.; Singh,S.; Pasricha, R.; Gupta, P.K.; Soni, D.; Patent Application; Publication Number US 8715612 B2, May 6, **2014**.
27. Cullity, B. D.; Stock S. R.; Elements of X-ray Diffraction, 3rd edition, Prentice Hall, **2001.**
DOI: 10.1098/rsif.2013.0319

